International Journal of Mathematical Archive-6(9), 2015, 133-146
Available online through www.ijma.info ISSN 2229 – 5046

EFFECT OF MAGNETIC, PERMEABILITY AND FORCHHEMIR PARAMETERS ON STEADY MHD FLOW OF NANOFLUID WITH ROTATION THROUGH NON-DARCY POROUS MEDIUM OVER EXPONENTIALLY STRETCHING POROUS SHEET

BHIM SEN KALA*[1], M. S. RAWAT[2], KOMAL[3]

[1]Dr. K. N. Modi Institute of Engineering and Technology, Modinagar, (U.P.), India.

[2,3]HNB Garhwal University Srinagar, Garhwal-246174, Uttarakhand, India.

(Received On: 31-08-15; Revised & Accepted On: 15-09-15)

ABSTRACT

In this paper, we discuss the effect of Magnetic, Permeability, and Forchhemir Parameters on the Steady Magnetohydrodynamic boundary layer flow of nanofluid over a continuous exponentially stretching porous surface through a Non-Darcy porous medium. By suitable similarity transformations, the governing boundary layer equations are transformed to ordinary differential equations and to solve these equations the method applied is numerical computation with bvp4c, a MATLAB program. The effects of various parameters like, Magnetic Parameter, Permeability Parameter, Forchheimer Parameter, Rotation Parameter etc. on velocity profiles, heat transfer, and nanoparticle volume fraction distribution, Skin- Frictions, Nusselt Number and Sherwood Number are computed and discussed numerically and presented through tables and graphs.

Keywords: *MHD Flow, Nanofluid , Permeability, Rotational Parameter, Forcheimer Parameter.*

1. INTRODUCTION

Historically, Crane [1] first studied the boundary layer flow due to linearly stretching sheet. Magyari and Keller [2] considered the boundary layer flow and heat transfer due to an exponentially stretching sheet. Bhattacharya and Pop [3] showed the effect of external magnetic field on the flow over an exponentially shrinking sheet.

In recent years studies on nanofluid heat and mass transfer boundary layer laminar flow have attracted considerable attention. Choi [4] introduced the technique of nanofluids by using a mixture of nanoparticles and the base fluids. The presence of the nanoparticles in the nanofluid increases the thermal conductivity and causes significant change in properties such as viscosity and specific heat in comparison to the base fluid. It has attracted many researchers to perform its engineering applications.

Shateyi, S. *et al.* [5] numerically investigated the magnetohydrodynamic boundary layer flow with heat and mass transfer of an incompressible upper-convected Maxwell fluid over a stretching sheet.

Ibrahim,S.M. *et al.* [6] analyzed numerically the mass transfer and thermal radiation on a steady two-dimensional laminar flow of a viscous incompressible electrically conducting micropolar fluid past a stretching surface embedded in a Non-Darcian porous medium in the presence of heat generation.

Nandy, S. K. [7] investigated the hydromagnetic boundary layer flow and heat transfer of a Non-Newtonian Casson fluid in the neighborhood of a stagnation point over a stretching surface in the presence of velocity and thermal slips at the boundary.

Corresponding Author: Bhim Sen Kala*[1]
[1]Dr. K. N. Modi Institute of Engineering and Technology, Modinagar, (U.P.), India.

Khan, W. A. *et al.* [8] numerically studied steady boundary layer flow past a stretching wedge with the velocity $u_w(x)$ in a nanofluid and with a parallel free stream velocity $u_e(x)$. Njane,W. N.M. et al. [9] studied the effect of magnetic field on boundary layer flow of an incompressible electrically conducting water-based nanofluid past a convectively heated vertical porous plate with Navier slip boundary condition. Goyal M. et al.[10] analyzed the effect of velocity slip boundary condition on the flow and heat transfer of Non-Newtonian nanofluid over a stretching sheet with a heat source/sink, under the action of a uniform magnetic field, orientated normally to the plate. Bhattacharyya K. et al. [11] presented a mathematical model of the steady boundary layer flow of nanofluid due to an exponentially permeable stretching sheet with external magnetic field.

Khan, Md.S. *et al.* [12] studied a two-dimensional steady flow of an electrically conducting, viscous incompressible nanofluid past a continuously moving surface in the presence of uniform transverse magnetic field with chemical reaction. Sheikholeslami, M. *et al.* [13] studied two-dimensional laminar-forced convection nanofluids flow over a stretching surface in a porous medium. Noghrehabadi, A. *et al.* [14] examined the combined effects of Brownian motion, thermophoresis, and magnetic field on the steady boundary-layer flow and heat transfer of nanofluids over a linear isothermal stretching sheet. Poornima T. *et al.* [15] presented the numerical solution of a steady free convective boundary-layer flow of a radiating nanofluid along a non-linear stretching sheet in the presence of transverse magnetic field.

Malvandi,A. *et al.* [16] dealt with the steady two-dimensional stagnation point flow of nanofluid toward an exponentially stretching sheet with nonuniform heat generation/absorption. Ferdows,M. *et al.* [17] studied Magnetohydrodynamic MHD boundary layer flow of a nanofluid over an exponentially stretching sheet. Hamad, M. A. A. *et al.* [18] analyzed the boundary-layer flow and heat transfer in a viscous fluid containing metallic nanoparticles over a nonlinear stretching sheet. Khan, Md. S, *et al.* [19] investigated numerically the study of mhd radiative heat transfer in a nanofluid within the influence of magnetic field over a stretching surface. Wahiduzzaman, M *et al.* [20] investigated numerically the viscous dissipation and radiative heat transfer in nanofluid with the influence of magnetic field over a rotating stretching surface.Takhar H.S. *et al.* [21] studied the flow and heat transfer on a stretching surface in a rotating fluid, in the presence of a magnetic field.

In the above mentioned works effect of rotational motion on flow of nanofluid over a continuous exponentially stretching porous surface through a non-Darcy porous medium is not considered.

Present paper deals with the study of effects of rotational motion on steady, free convective MHD Nanofluid flow and heat and mass transfer over an Exponentially Stretching Sheet embedded in a Non-Darcy porous medium with heat source. Using similarity transformations the governing boundary layer equations are transformed to the ordinary differential equations. The computed results are discussed in detail with table and graphical representation.

2. MATHEMATICAL MODEL FORMULATION

Consider the steady boundary layer flow with rotational (angular) motion past a stretching surface in a porous medium filled with a nanofluid. The magnetic Reynolds number is assumed to be small, so that the induced magnetic field is negligible. The fluid is assumed to be electrically non-conducting. The convecting fluid and the porous medium are everywhere in thermodynamic equilibrium. It is assumed that the uniform temperature of the surface is T_w and that of the nanofluid volume fraction is C_w; the uniform temperature and nanofluid volume fraction in the ambient (free flow region) fluid are T_∞ and C_∞ respectively. There is no rotational motion of the ambient (free flow region) fluid. It is also assumed that the plate is exponentially stretched with a velocity $u_w(x) = c\exp\left(\frac{x}{L}\right)$, where c is a positive constant and having no initial rotational motion. The flow is assumed to be high so that an advective term and a Forchheimer quadratic drag term do appear in the momentum equations. The viscous dissipation and radiation terms have not been taken into account. The Physical Model of the problem with coordinate system is as shown in the Figure 1.

Under these assumptions, the following five field equations embodying the conservation of total mass, momentum (Brinkman-Forchheimer equations), energy and nanofluid volume fraction equations for the nanofluid are considered as follows.

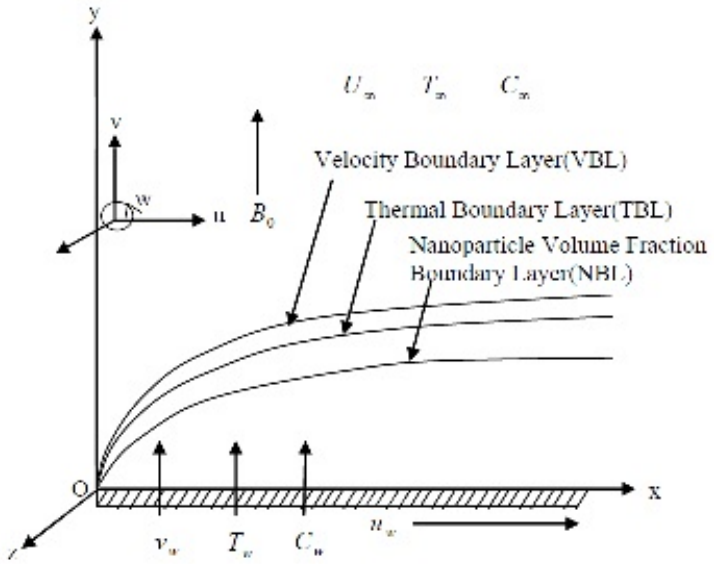

Figure 1: Physical model and coordinate system.

The Equation of Continuity:

$$\frac{\partial u}{\partial x}+\frac{\partial u}{\partial y}=0. \tag{2.1}$$

The Equation of Momentum:

$$u\frac{\partial u}{\partial x}+\upsilon\frac{\partial u}{\partial y}=\nu\frac{\partial^2 u}{\partial y^2}-\frac{\sigma B_0^2}{\rho_f}u-\frac{\mu}{K}u-\frac{b}{\sqrt{K}}u^2+2\Omega w. \tag{2.2}$$

The Equation of Angular Momentum

$$u\frac{\partial w}{\partial x}+\upsilon\frac{\partial w}{\partial y}=\nu\frac{\partial^2 w}{\partial y^2}-\frac{\sigma B_0^2}{\rho_f}w-\frac{\mu}{K}w-\frac{b}{\sqrt{K}}w^2-2\Omega u. \tag{2.3}$$

The Equation of Energy:

$$u\frac{\partial T}{\partial x}+\upsilon\frac{\partial T}{\partial y}=\alpha\frac{\partial^2 T}{\partial y^2}+\frac{Q_x}{\rho c_p}(T-T_\infty)+\frac{(\rho C)_p}{(\rho C)_f}\left(D_B\frac{\partial C}{\partial y}\frac{\partial T}{\partial y}+\frac{D_T}{T_\infty}\left(\frac{\partial T}{\partial y}\right)^2\right). \tag{2.4}$$

The Equation of Mass:

$$u\frac{\partial C}{\partial x}+\upsilon\frac{\partial C}{\partial y}=D_B\frac{\partial^2 C}{\partial y^2}+\frac{D_T}{T_\infty}\frac{\partial^2 T}{\partial y^2}. \quad , \tag{2.5}$$

where x and y are Cartesian coordinates along the stretching wall and normal to it respectively. u and v are the velocity components along the x-and y-axes and w being rotational velocity about normal to x-y plane i.e. about z axis. T is the temperature in the fluid phase. C is the nanoparticle volume fraction. $B(x)=B_0\exp\left(\frac{x}{2L}\right)$ is variable magnetic field and B_0 is constant. K is the permeability of the porous medium. b is For chheimer coefficient. Ω is coefficient of rotational motion. ρ,ν and μ are the density, kinematic viscosity and dynamic viscosity of the fluid, respectively.

Further, $(\rho C_p)_f$ is the heat capacity of the fluid. $(\rho C_p)_p$ is the effective heat capacity of the nanoparticle material and α is the effective thermal conductivity of the porous medium. The coefficients that appear in (2.4) and (2.5) are the heat source coefficient Q_x , the Brownian diffusion coefficient D_B and the thermophoretic diffusion coefficient D_T.

The boundary conditions for (2.1) – (2.5) are:

$$\left.\begin{aligned} &y=0: u=u_w(x)=c\exp\left(\frac{x}{L}\right),\ \upsilon=\upsilon_w, w(x,0)=0 \\ &T=T_w=T_\infty+T_0\exp\left(\frac{x}{2L}\right),\ C=C_w=C_\infty+C_0\exp\left(\frac{x}{2L}\right); \\ &y\to\infty: u\to 0, w(x,y)\to 0, T\to T_\infty, C\to C_\infty, \\ &where\ u_w(x)=c\exp\left(\frac{x}{L}\right),\ \upsilon_w(x)=c\exp\left(\frac{x}{2L}\right). \end{aligned}\right\} \tag{2.6}$$

Dimensional Analysis:

We define

$$\left.\begin{aligned} &\eta=\left(\frac{c}{2\nu L}\right)^{\frac{1}{2}}e^{\frac{x}{2L}}y,\ \psi=(2\nu Lc)^{\frac{1}{2}}e^{\frac{x}{2L}}f(\eta),\ \theta(\eta)=\frac{(T-T_\infty)}{(T_w-T_\infty)}, \\ &\phi(\eta)=\frac{(C-C_\infty)}{(C_w-C_\infty)}, u=\frac{\partial\psi}{\partial y}, \upsilon=-\frac{\partial\psi}{\partial x}, w(\mathrm{x},\mathrm{y})=\mathrm{c}\,e^{\frac{x}{L}}\mathrm{g}(\eta). \end{aligned}\right\} \tag{2.7}$$

Here η is similarity variable, ψ is a stream function. θ is non-dimensional Temperature. ϕ is non-dimensional concentration.

Using (2.7) in (2.2)-(2.5) can be written as

$$f'''+ff''-2(f')^2-\left(\left(M+\frac{1}{K1}\right)f'+Fs(f')^2\right)+R1g=0 \tag{2.8}$$

$$g''+fg'-2f'g-R1f'-\left(\left(M+\frac{1}{K1}\right)g+Fs(g)^2\right)=0 \tag{2.9}$$

$$\theta''+\mathrm{Pr}(f\theta'-f'\theta+\lambda\theta+Nb\theta'\phi'+Nt(\theta')^2)=0 \tag{2.10}$$

$$\phi''+Le\left(f\phi'-f'\phi\right)+\frac{Nt}{Nb}\theta''=0 \tag{2.11}$$

and boundary conditions (2.6) as

$$\left.\begin{aligned} &f(0)=S,\ f'(0)=1,\theta(0)=1,\phi(0)=1,g(0)=0. \\ &f'(\eta)\to 0,\theta(\eta)\to 0,\phi(\eta)\to 0,g(\eta)\to 0\ \ as\ \eta\to\infty. \end{aligned}\right\} \tag{2.12}$$

where $S=-\upsilon_0/\sqrt{c\nu/2L}$ is the wall mass transfer parameter.

$S>0$ $(\upsilon_0<0)$ corresponds to mass suction and $S<0$ $(\upsilon_0>0)$ corresponds to mass injection .

Here prime denotes differentiation with respect to η.

The parameters occurring in (2.8) to (2.11) are defined as follows

$$\left.\begin{aligned} &M=\frac{2\sigma B_0^2L}{\rho_f c}e^{-\frac{x}{L}}, K1=\frac{Kce^{\frac{x}{L}}}{2L\nu}, Fs=\frac{2bL}{\sqrt{K}}, \mathrm{Pr}=\frac{\nu}{\alpha}, \alpha=\frac{k}{\rho C_p}, Le=\frac{\nu}{D_B}, \\ &Nb=D_B\frac{(\rho C)_p}{(\rho C)_f}\frac{(C_w-C_\infty)}{\nu}, Nt=\frac{D_T}{T_\infty}\frac{(\rho C)_p}{(\rho C)_f}\frac{(T_w-T_\infty)}{\nu}, \nu=\frac{\mu}{\rho}, \\ &Q_x=\lambda(c/2L)e^{x/L}, R1=4\Omega L/\mathrm{U}, \mathrm{U}=ce^{x/L}. \end{aligned}\right\} \tag{2.13}$$

$Q_x = \lambda(c/2L)e^{x/L}$ is the nonuniform heat generation/absorption coefficient where $\lambda > 0$ and $\lambda < 0$ stand for heat generation and absorption parameters respectively. R1 is fluid rotational parameter. $U = ce^{x/L}$ is the fluid velocity depending exponentially upon x.

The quantities of physical interest for this problem are the local Skin-friction due to linear motion (C_f), local Skin-friction due to rotation (C_g), local Nusselt number (Nu_x) , local Sherwood Number (Sh_x) and local Reynold Number (Re_x).These are defined as follows:

$$\left.\begin{aligned} C_f &= \frac{\tau_w}{\frac{\rho U_w^2}{2}} = \frac{\mu\left(\frac{\partial u}{\partial y}\right)_{y=0}}{\frac{\rho U_w^2}{2}} \Rightarrow C_f = \frac{1}{\sqrt{2\,\mathrm{Re}_x}} f''(0), \\ C_g &= -\frac{1}{\sqrt{2\,\mathrm{Re}_x}} g'(0),\ \mathrm{Re}_x = u_w x/\nu \\ Nu_x &= -\frac{x\left(\frac{\partial T}{\partial y}\right)_{y=0}}{T_w - T_\infty} = -\sqrt{\frac{x}{L}\mathrm{Re}_x}\ \theta'(0), \\ \mathrm{Sh}_x &= -\frac{x\left(\frac{\partial C}{\partial y}\right)_{y=0}}{C_w - C_\infty} = -\sqrt{\frac{x}{L}\mathrm{Re}_x}\ \varphi'(0). \end{aligned}\right\} \quad (2.14)$$

3. METHOD OF NUMERICAL SOLUTION

The numerical solutions are obtained using the above equations for some values of the governing parameters, namely, the Magnetic Parameter (*M*), the Permeability Parameter (K1), the Forchheimer Parameter (Fs), Rotational Parameter (R1). Effects of *M*, K1, Fs, R1 on the steady boundary layer flow are discussed in detail. The numerical computation is done using the MATLAB in-built Numerical Solver bvp4c. In the computation we have taken $\eta_\infty = 10$ and axis according to the clear figure-visuality.

4. RESULT AND DISCUSSION

The nondimensional linear velocity $f'(\eta)$, rotational velocity $g(\eta)$, temperature $\theta(\eta)$, and nanoparticle volume fraction $\phi(\eta)$ for various values of different parameters are shown in Figures 2 to 17.

To ensure the numerical accuracy, the values $f''(0)$ and $f(\infty)$ by present method are compared with the results of Magyari and Keller [18] and Krishnendu Bhattacharyya and G. C. Layek [7] in Table 1 without magnetic field ($M = 0$) , non porous media (K1=0, Fs=0) and having no rotational motion (R1=0) and with nonporous stretching sheet ($S = 0$) and those are found in excellent agreement. Thus, we are very much confident that the present results are accurate.

Table1: The comparison of values of $-f''(0)$ and $f(\infty)$ for M=0; K1=inf; Fs=0.0; R1=0.00; S=0.0;Pr=0.7; Q1=0.5; Le=2; Nt=0.5; Nb=0.5.

	Magyari and Keller [18]	Krishnendu Bhattacharyya and G. C. Layek[7]	Present study
$-f''(0)$	-1.281808	-1.28180838	-1.281817759582543
$f(\infty)$	0.905639	0.90564328	0.905021224296639

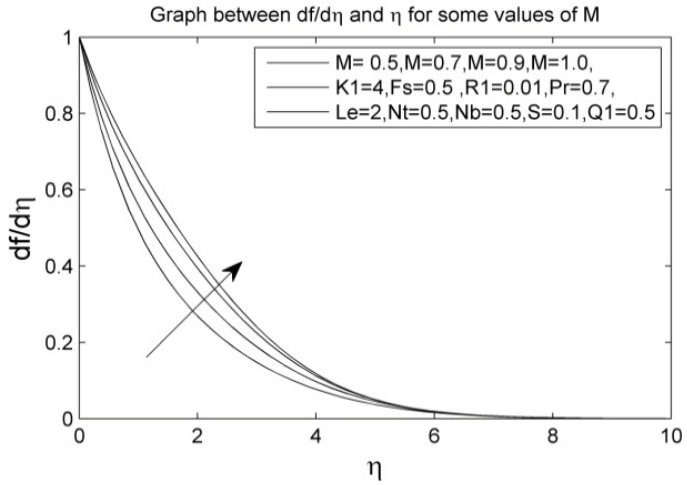

Figure 2: Graph between $f'(\eta)$ and η for some values of M.

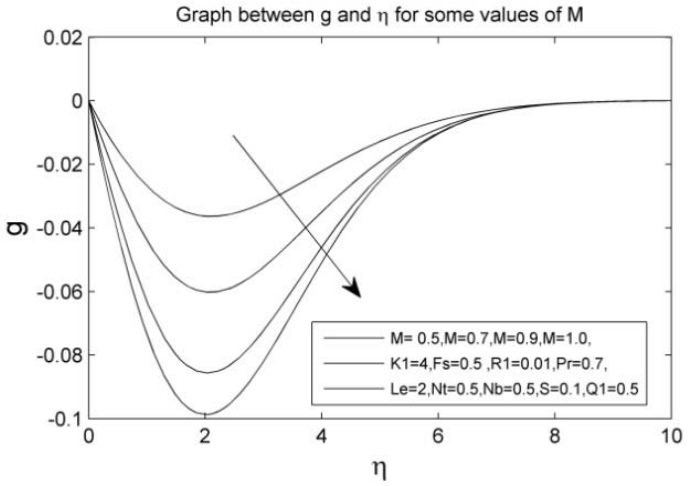

Figure 3: Graph between $g(\eta)$ and η for some values of M.

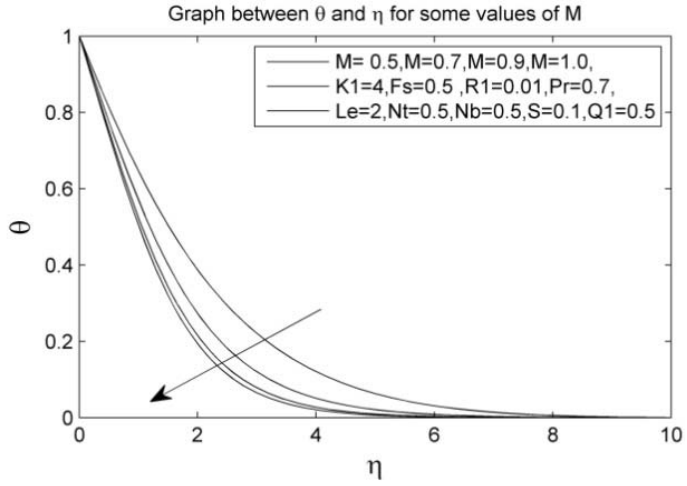

Figure 4: Graph between $\theta(\eta)$ and η for some values of M.

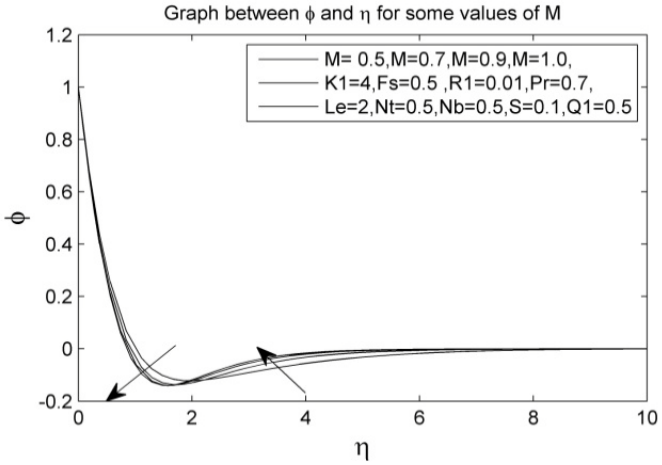

Figure 5: Graph between $\phi(\eta)$ and η for some values of M.

The nondimensional translational velocity $f'(\eta)$, angular (rotational) velocity, $g(\eta)$ temperature $\theta(\eta)$ and nanoparticle volume fraction, $\phi(\eta)$ for various values of magnetic parameter M, are shown in Figure 2 to 5. In the presence of mass suction $S > 0$ $(\upsilon_0 < 0)$, the velocity increases with the increase of magnetic parameter. The magnetic field favours the transport process. The increase of *M* leads to the decrease of the Lorentz force which is due to interaction of magnetic and electric fields in the motion of an electrically conducting fluid. The stronger Lorentz force produces lesser resistance to the transport phenomena. Angular velocity of fluid decreases. Also, the temperature and the nanoparticle volume fraction decrease with *M*. The Lorentz force has the tendency to decrease the temperature and nanoparticle volume fraction in nanofluid motion. Consequently, velocity boundary layer thickness becomes thicker and angular velocity boundary layer thickness, the thermal boundary layer thickness and nanoparticle volume fraction boundary thickness become thiner for stronger magnetic field.

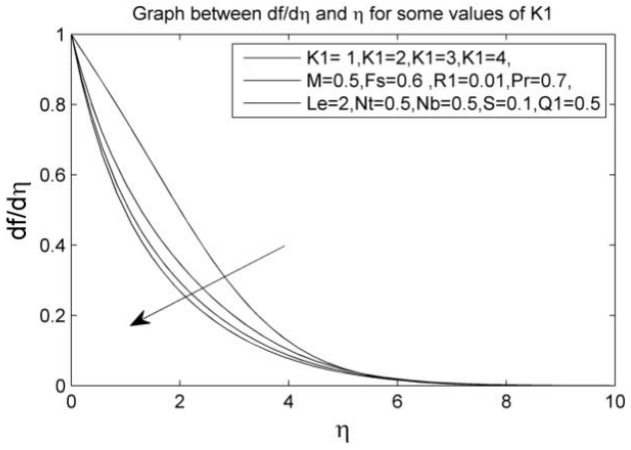

Figure 6: Graph between $f'(\eta)$ and η for some values of K1.

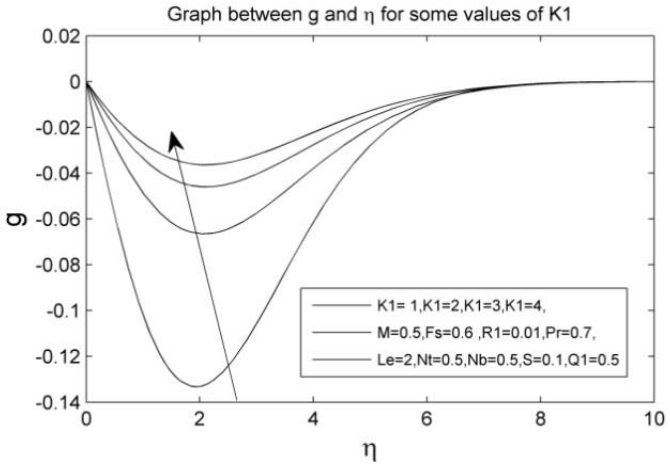

Figure 7: Graph between $g(\eta)$ and η for some values of K1.

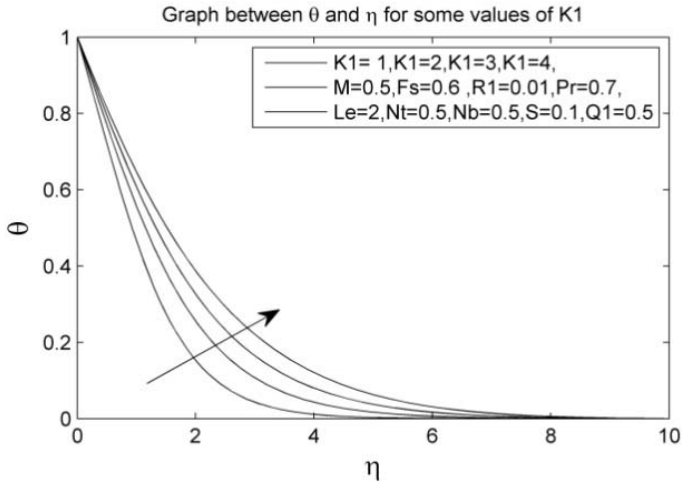

Figure 8: Graph between $\theta(\eta)$ and η for some values of K1.

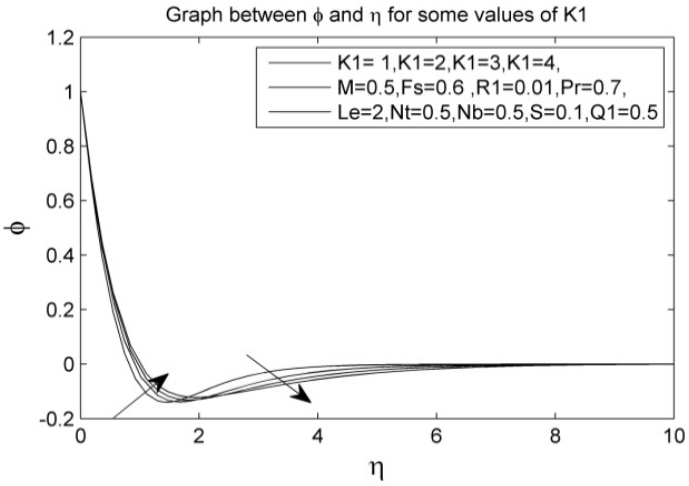

Figure 9: Graph between $\phi(\eta)$ and η for some values of K1.

The nondimensional translational velocity $f'(\eta)$, angular (rotational) velocity $g(\eta)$, temperature $\theta(\eta)$ and nanoparticle volume fraction $\phi(\eta)$, for various values of porosity parameter K1 are shown in Figure 6 to 9. The velocity decreases with the increase of porosity parameter K1. On the other hand, the angular velocity of the fluid, the temperature and the nanoparticle volume fraction increase with K1. Consequently, velocity boundary layer thickness becomes thinner and angular velocity boundary layer thickness, the thermal boundary layer thickness and nanoparticle volume fraction boundary thickness become thicker for larger K1.

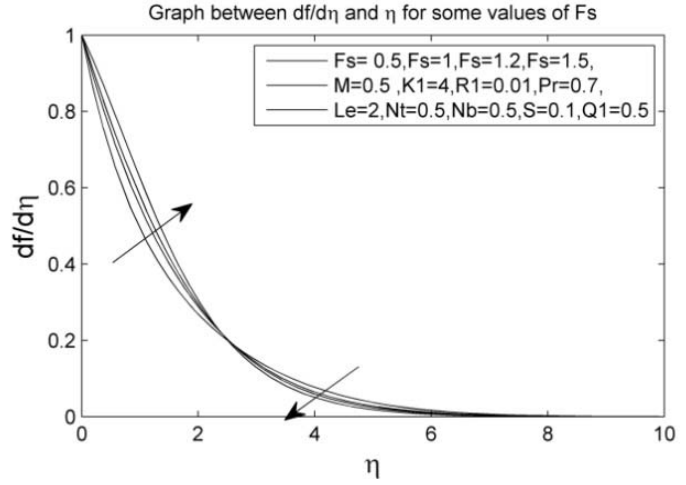

Figure 10: Graph between $f'(\eta)$ and η for some values of Fs.

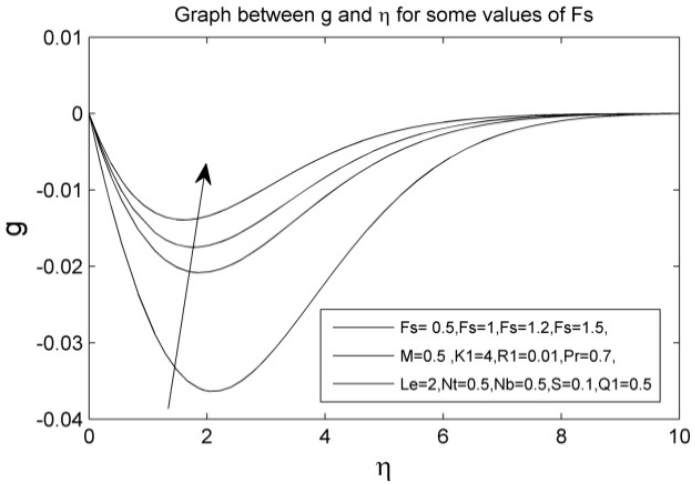

Figure 11: Graph between $g(\eta)$ and η for some values of Fs.

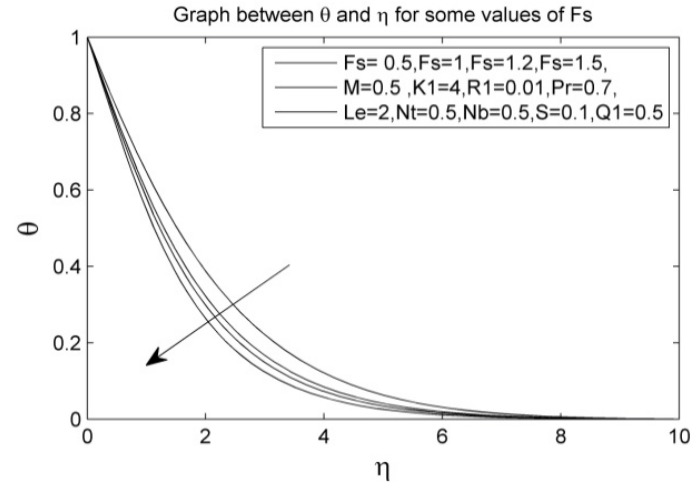

Figure 12: Graph between $\theta(\eta)$ and η for some values of Fs.

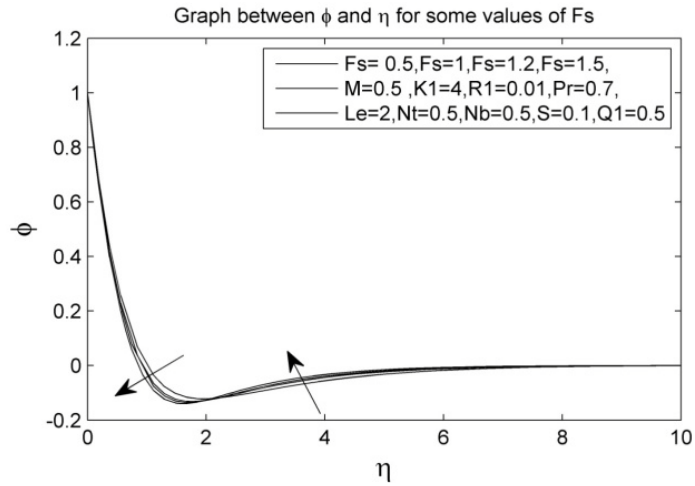

Figure 13: Graph between $\phi(\eta)$ and η for some values of Fs.

The nondimensional translational velocity $f'(\eta)$, angular (rotational) velocity $g(\eta)$, temperature $\theta(\eta)$ and nanoparticle volume fraction $\phi(\eta)$, for various values of Forchheimer parameter Fs, are shown in Figure 10 to 13. The linear velocity and the angular velocity of the fluid increase with the increase of Forchheimmer parameter Fs. On the other hand, the temperature and the nanoparticle volume fraction decrease with Fs. Consequently, velocity boundary layer thickness and angular velocity boundary layer thickness become thicker, and the thermal boundary layer thickness and nanoparticle volume fraction boundary thickness become thinner for larger Fs.

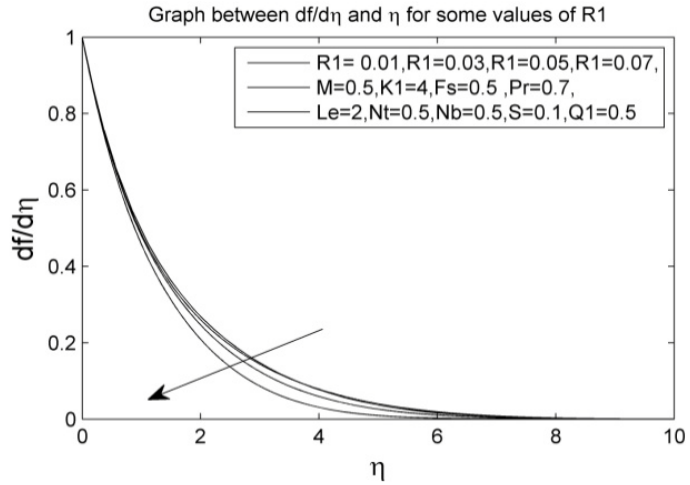

Figure 14: Graph between $f'(\eta)$ and η for some values of R1.

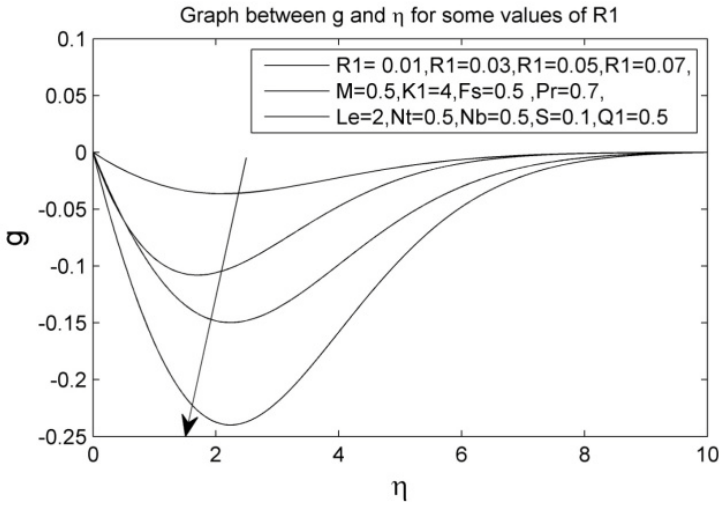

Figure 15: Graph between $g(\eta)$ and η for some values of R1.

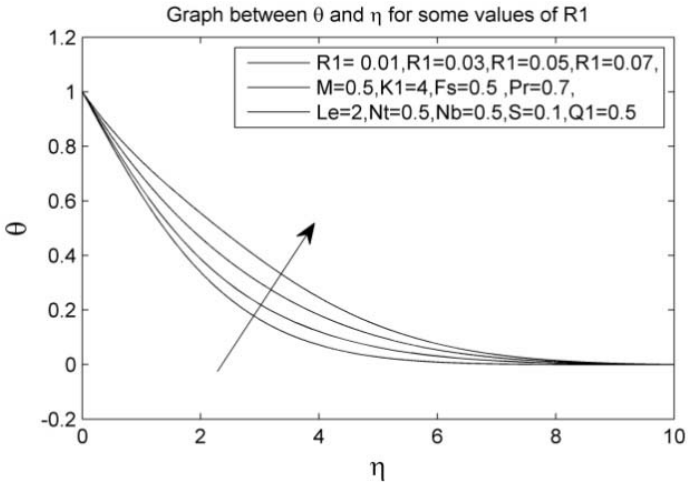

Figure 16: Graph between $\theta(\eta)$ and η for some values of R1.

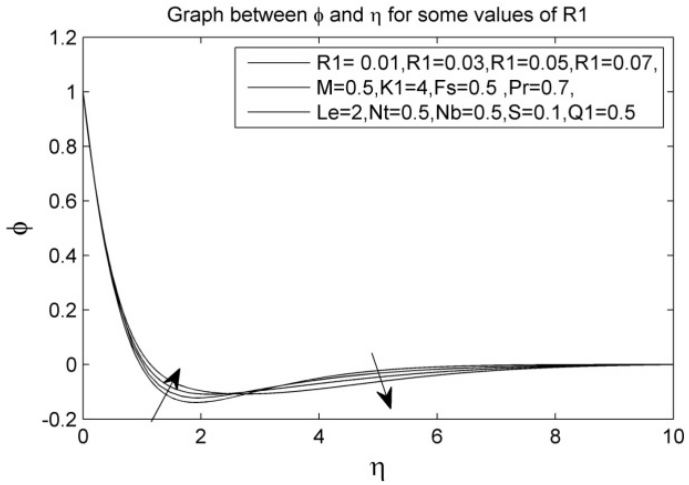

Figure 17: Graph between $\phi(\eta)$ and η for some values of R1.

The nondimensional translational velocity $f'(\eta)$, angular (rotational) velocity $g(\eta)$, temperature $\theta(\eta)$ and nanoparticle volume fraction $\phi(\eta)$, for various values of rotation parameter R1 are shown in Figure 14 to 17. The linear velocity and the angular velocity of the fluid decrease with the increase of rotation parameter R1. On the other hand, the temperature and the nanoparticle volume fraction increase with R1. Consequently, velocity boundary layer thickness and angular velocity boundary layer thickness become thinner, and the thermal boundary layer thickness and nanoparticle volume fraction boundary thickness become thicker for larger R1.

We now discuss the variations of the physical quantities of engineering importance, that is, the local Skin Friction coefficient for Linear velocity Cf, local Skin Friction coefficient for Rotational velocity and the local Nusselt Number Nux, local Sherwood Number for different values of M,K1,Fs, and R1. The quantities $f''(0)$, $g'(0)$, $\theta'(0)$ and $\phi'(0)$ related to local skin friction coefficient for linear velocity C_f, local Skin Friction coefficient for Rotational velocity C_g, the local Nusselt Number Nu_x, local Sherwood Number Sh_x are given in tables 2 to 5 for various values of parameters.

Table2. Table for $f''(0)$, $g'(0)$, $\theta'(0)$ and $\phi'(0)$ for different values of M at K1=4; Fs=0.5; R1=0.01; Pr=0.7; Q1=0.5; Le=2; Nt=0.5; Nb=0.5; S=0.1.

M	$f''(0)$	$g'(0)$	$\theta'(0)$	$\phi'(0)$
0.5	-0.791430508416108	-0.036562717806286	0.388468637335052	1.929810650727245
0.7	-0.65590885665634	-0.056357886100721	0.453195784609117	1.965568409675726
0.9	-0.511550410652045	-0.079375624184983	0.494134375485658	1.996733798027171
1.0	-0.436341405600862	-0.091974854928743	0.511342208881025	2.011880484551393

Table 2 shows $f''(0)$ increases, $g'(0)$ decreases, $\theta'(0)$ and $\phi'(0)$ increase with M.

Table 3. Table for $f''(0)$, $g'(0)$, $\theta'(0)$ and $\phi'(0)$ for different values of K1 at M=0.5; Fs=0.5; R1=0.01; Pr=0.7; Q1=0.5; Le=2; Nt=0.5; Nb=0.5; S=0.1.

K1	$f''(0)$	$g'(0)$	$\theta'(0)$	$\phi'(0)$
1	-0.240055296498474	-0.12719692346525	0.549168474142145	2.049122117082349
2	-0.62060635671019	-0.061844512535624	0.464574800279222	1.973530711812985
3	-0.736115884241243	-0.044331924755409	0.421141880698140	1.945982263247798
4	-0.791430508416108	-0.036562717806286	0.388468637335052	1.929810650727245

Table 3 shows $f''(0)$ decreases, $g'(0)$ increases, $\theta'(0)$ and $\phi'(0)$ decrease with K1.

Table 4. Table for $f''(0), g'(0), \theta'(0)$ and $\phi'(0)$ for different values of Fs at M=0.5; K1=4; R1=0.01; Pr=0.7; Q1=0.5; Le=2; Nt=0.5; Nb=0.5; S=0.1.

Fs	$f''(0)$	$g'(0)$	$\theta'(0)$	$\phi'(0)$
0.5	-0.791430508416108	-0.036562717806286	0.388468637335052	1.929810650727245
1.0	-0.578881594882092	-0.025952316333218	0.435136868976853	1.981551072522049
1.2	-0.481390515281348	-0.023712331368310	0.453626495246452	2.003499800165463
1.5	-0.316741480029212	-0.021346501616894	0.482261100630321	2.038717191165877

Table 4 shows $f''(0), g'(0), \theta'(0)$ and $\phi'(0)$ increase with Fs.

Table 5. Table for $f''(0), g'(0), \theta'(0)$ and $\phi'(0)$ for different values of R1 at M=0.5; K1=4; Fs =0.5; Pr=0.7; Q1=0.5; Le=2; Nt=0.5; Nb=0.5; S=0.1.

R1	$f''(0)$	$g'(0)$	$\theta'(0)$	$\phi'(0)$
0.01	-0.791430508416108	-0.036562717806286	0.388468637335052	1.929810650727245
0.03	-0.804978525572459	-0.135249878530288	0.352626085770798	1.923001471550448
0.05	-0.828256354045100	-0.217706260536009	0.310306707747155	1.915054081886551
0.07	-0.801568530938947	-0.153058432606265	0.407476801754900	1.930819622637134

Table5 shows $f''(0), g'(0), \theta'(0)$ and $\phi'(0)$ decrease with R1 for its first three values while increase at its fourth value.

5. CONCLUSION

In this paper, we have studied the Steady Magnetohydrodynamic boundary layer flow of nanofluid over a continuous exponentially stretching porous surface through a Non-Darcy porous medium and discussed the effect of Magnetic, Permeability, and Forchhemir parameters etc. on velocity profiles, heat transfer and nanoparticle volume fraction distribution. Skin Frictions, Nusselt Number and Sherwood Number are computed and discussed numerically and presented through tables and graphs.

Figures 2 to 17 show following results:

The nondimensional translational velocity $f'(\eta)$ increases with the increase of magnetic parameter M and Forchheimer parameter Fs. Consequently, velocity boundary layer thickness becomes thicker for larger M and Fs.

The angular (rotational) velocity $g(\eta)$ increases with the increase of porosity parameter K1 and Forchheimer parameter Fs. Consequently, angular velocity boundary layer thickness becomes thicker for larger K1 and Fs.

The temperature increases with porosity parameter K1 and rotation parameter R1. Consequently, the thermal boundary layer thickness becomes thicker for larger K1 and R1.

The nanoparticle volume fraction increases with porosity parameter K1 and rotation parameter R1. Consequently, nanoparticle volume fraction boundary thickness become thicker for larger K1 and R1.

The nondimensional translational velocity $f'(\eta)$ decreases with the increase of porosity parameter K1 and rotation parameter R1. Consequently, velocity boundary layer thickness becomes thinner for larger K1 and R1.

The angular (rotational) velocity $g(\eta)$ decreases with the increase of magnetic parameter M and rotational parameter R1. Consequently, angular velocity boundary layer thickness becomes thicker for larger M and R1.

The temperature $\theta(\eta)$ decrease with magnetic parameter M and Forchheimer parameter Fs. Consequently, the thermal boundary layer thickness become thinner for larger M and Fs.

The nanoparticle volume fraction $\phi(\eta)$ decrease with the increase of magnetic parameter M and Forchheimer parameter Fs.. Consequently, nanoparticle volume fraction boundary thickness become thinner for larger M and Fs.

Tables 2 to 5 show following results:

$f''(0)$ increases with M and Fs; $g'(0)$ increases with K1 and Fs; $\theta'(0)$ increases with M and Fs ; $\phi'(0)$ increases with M and Fs.

$f''(0)$, $\theta'(0)$ and $\phi'(0)$ decrease with K1; $g'(0)$ decreases with M.

$f''(0)$, $g'(0)$, $\theta'(0)$ and $\phi'(0)$ decrease with R1 for its first three values while increase at its fourth value.

COMPETING INTERESTS

The authors declare that they have no competing interests.

ACKNOWLEDGEMENT

I am thankful to Prof. D.S.Negi Head, Department of Mathematics, HNB Garhwal University, for his support during the preparation of the paper.

REFERENCE

1. Crane, L. J.(1970). Flow past a stretching plate. *Zeitschrift f¨ur Angewandte Mathematik und Physik ZAMP, vol. 21, no. 4, pp. 645–647, 1970.*
2. E. Magyari and B. Keller(1999). Heat and mass transfer in the boundary layers on an exponentially stretching continuous surface. *Journal of Physics D*, vol. 32, no. 5, pp. 577–585, 1999.
3. Bhattacharyya, K. and Pop, I. (2011).Mhd boundary layer flow due to an exponentially shrinking sheet. *Magnetohydrodynamics, vol. 47, pp. 337–344, 2011.*
4. Choi, S. U. S.(1995). Enhancing thermal conductivity of fluids with nanoparticles. *Proceedings of the ASME International Mechanical Engineering Congress and Exposition, vol. 66, pp. 99–105, San Francisco, Calif, USA, November 1995.*
5. Shateyi, S. and G. T.Marewo,(2013).A New Numerical Approach of MHD Flow with Heat and Mass Transfer for the UCM Fluid over a Stretching Surface in the Presence of Thermal Radiation. *Hindawi Publishing Corporation,Mathematical Problems in Engineering Volume 2013, Article ID 670205, 8 pages* .
6. Ibrahim, S. M., T. S. Reddy, and N. B. Reddy (2013). Radiation and Mass Transfer Effects on MHD Free Convection Flow of a Micropolar Fluid past a Stretching Surface Embedded in a Non-Darcian Porous Medium with Heat Generation. *.ISRN Thermodynamics, Volume 2013, Article ID 534750, 15 pages.*
7. Nandy, S.K. (2013). Analytical Solution of MHD Stagnation-Point Flow and Heat Transfer of Casson Fluid over a Stretching Sheet with Partial Slip. *Hindawi Publishing Corporation ISRN Thermodynamics, Volume* 2013, *Article ID 108264, 9 pages.*
8. Khan, W. A. and I. Pop (2013). Boundary Layer Flow Past a Wedge Moving in a Nanofluid' *Hindawi Publishing Corporation Mathematical Problems in Engineering, Volume2013, Article ID 637285, 7 pages.*
9. Njane, W. N. and O. Daniel (2013) Combined Effect of Buoyancy Force and Navier Slip on MHD Flow of a Nanofluid over a Convectively Heated Vertical Porous Plate. *Hindawi Publishing Corporation, The ScientificWorld Journal , Volume 2013, Article ID 725643, 8 pages.*
10. Goyal, M. and Rama Bhargava (2013). Numerical Solution of MHD Viscoelastic Nanofluid Flow over a Stretching Sheet with Partial Slip and Heat Source/Sink. *Hindawi Publishing Corporation, ISRN Nanotechnology, Volume 2013, Article ID 931021, 11 pages.*
11. Bhattacharyya K. and G. C. Layek, (2014). Magnetohydrodynamic Boundary Layer Flow of Nanofluid over an Exponentially Stretching Permeable Sheet. *Hindawi Publishing Corporation, Physics Research International, Volume 2014, Article ID 592536, 12 pages.*
12. Khan, Md. S., I. Karim and Md. S. Islam(2014).Possessions of Chemical Reaction on MHD Heat and Mass Transfer Nanofluid Flow on a Continuously Moving Surface. *American Chemical Science Journal 4(3): 401-415.*
13. Sheikholeslami, M. and D. D. Ganji.(2014). Heated Permeable Stretching Surface in a Porous Medium Using Nanofluids. *Journal of Applied Fluid Mechanics*, Vol. 7, No. 3, pp. 535-542. Available online at www.jafmonline.net, ISSN 1735-3572, EISSN 1735-3645.
14. Noghrehabadi, A., M. Ghalambaz, and A. Ghanbarzadeh.(2012). Heat Transfer of Magnetohydrodynamic Viscous Nanofluids over an Isothermal Stretching Sheet. *JOURNAL OF THERMOPHYSICS AND HEAT TRANSFER Vol. 26, No. 4.*

15. Poornima, T. and N. B. Reddy. (2013). Radiation effects on MHD free convective boundary layer flow of nanofluids over a nonlinear stretching sheet. *Advances in Applied Science Research, 2013, 4(2):190-202.*
16. Malvandi, A., F. Hedayati, and G. Domairry.(2013). Stagnation Point Flow of a Nan fluid toward an Exponentially Stretching Sheet with Nonuniform Heat Generation/Absorption. *Hindawi Publishing Corporation Journal of Thermodynamics, Volume 2013, Article ID 764827, 12 pages*.
17. http://dx.doi.org/10.1155/2013/764827.
18. Ferdows, M., Md. S. Khan, Md. M. Alam, and S.Sun.(2012). MHD Mixed Convective Boundary Layer Flow of a Nanofluid through a Porous Medium due to an Exponentially Stretching Sheet. *Hindawi Publishing Corporation, Mathematical Problems in Engineering, Volume 2012, Article ID 408528, 21 pages*. doi:10.1155 /2012/408528.
19. Hamad, M. A. A., M. Ferdows. (2012).Similarity solutions to viscous flow and heat transfer of nanofluid over nonlinearly stretching sheet..*Appl. Math. Mech. -Engl. Ed., 33(7), 923–930 (2012).* DOI 10.1007/s10483-012-1595-7.
20. Khan, Md. Shakhaoath, Md. M. Alam, and M. Ferdows.(2011). MHD Radiative Boundary Layer Flow of a Nanofluid past a Stretching Sheet. *Proceedings of the International Conference on Mechanical Engineering and Renewable Energy 2011, (ICMERE2011) 22- 24 December 2011, Chittagong, Bangladesh*
21. Wahiduzzaman, M., Md. Shakhaoath Khan, P. Biswas, Ifsana Karim, M. S. Udd.(2015).Viscous Dissipation and Radiation Effects on MHD Boundary Layer Flow of a Nanofluid Past a Rotating Stretching Sheet. *Applied Mathematics, 2015, 6, 547-567.* http://dx.doi.org/10.4236/am.2015.63050.
22. Takhar, H.S. , A.J. Chamkha , G. Nath.(2003).Flow and heat transfer on a stretching surface in a rotating fluid with a magnetic field. *International Journal of Thermal Sciences 42 (2003) 23–31*.

Source of support: Nil, Conflict of interest: None Declared